Am J Cancer Res 2022;12(1):381-395
www.ajcr.us /ISSN:2156-6976/ajcr0140822

Original Article

Trastuzumab aggravates radiation induced cardiotoxicity in mice

Peiqiang Yi[1*], Huan Li[1*], Jun Su[1], Jialin Cai[2], Cheng Xu[1], Jiayi Chen[1], Lu Cao[1], Min Li[1]

[1]Department of Radiation Oncology, Ruijin Hospital, Shanghai Jiaotong University School of Medicine, Shanghai, China; [2]Clinical Research Center, Ruijin Hospital, Shanghai Jiaotong University School of Medicine, Shanghai, China. [*]Equal contributors.

Received November 28, 2021; Accepted December 30, 2021; Epub January 15, 2022; Published January 30, 2022

Abstract: Some breast cancer patients with overexpression of human epidermal growth factor receptor 2 need both chest radiotherapy and targeted therapy with trastuzumab (TRZ). The cardiotoxicity associated with combined treatment potentially restricts the clinical benefits of antitumor therapy. There is no consensus on whether and how chest radiotherapy can be given in concurrent with TRZ at present, considering the cardiotoxicity. This study intends to establish an *in vitro* and *in vivo* heart injury model by irradiation and TRZ, analyze whether there is a synergistic effect in heart, and to explore the molecular changes. First, an *in vitro* irradiation model of H9C2 cardiomyocytes was established. The effects of TRZ and radiation on cardiomyocyte injury were observed by cell flow cytometry, CCK-8 test, Western blot, γ-H2AX fluorescence focus formation and cell Reactive Oxygen Species (ROS) content test. Second, the mouse heart injury model was set up by X-ray cardiac irradiation combined with TRZ. Six months later, the cardiac function was analyzed by small animal ultrasound and ^{18}FDG-micro PET/CT. The morphological changes of heart tissue were assessed by histological section. We found that concurrent TRZ aggravates the injury effect of irradiation on cardiomyocytes *in vitro*. The influence of TRZ might be consequence of inhibiting Akt phosphorylation, promoting the excessive accumulation of ROS in cells and promoting intracellular DNA damage. In animal experiments, the dysfunction of diastolic and myocardial ischemia of mouse heart was observed by echocardiography and ^{18}FDG-micro PET/CT, respectively; myocardial fibrosis and cardiomyocyte apoptosis were also observed. Therefore, our *in vitro and in vivo* experiments have revealed that TRZ combined irradiation caused more cardiotoxicity than irradiation or TRZ alone. These results suggested that the concurrent management of TRZ and radiotherapy should be carefully made in clinical practice, and more attention is needed on cardiac safety.

Keywords: Trastuzumab, radiation, cardiotoxicity, heart, mice

Introduction

Radiotherapy is an indispensable part of comprehensive anti-cancer therapy. More than 50% of tumor patients need radiotherapy in the process of treatment [1]. Although chest irradiation significantly improved disease-free survival time in patients with thoracic tumors (including breast cancer, lung cancer, esophageal cancer, Hodgkin lymphoma), the long-term overall survival of these patients is impacted by the related radiation-induced cardiovascular toxicity [2, 3]. Cardiovascular adverse events are the most common cause of long-term non-tumor deaths in patients with Hodgkin lymphoma and breast cancer after radiotherapy [4, 5]. Therefore, the cardiovascular toxicity must be carefully considered in the process of receiving chest radiotherapy.

Overexpression of human epidermal growth factor receptor 2 (HER-2) occurs in 25-30% of breast cancer patients. HER-2 positive patients benefited from trastuzumab (TRZ) treatment because it specifically binds to HER-2 receptors [6]. However, the most noteworthy adverse effect of TRZ is cardiotoxicity [7]. The treatment course of TRZ often overlapped with that of radiotherapy in breast cancer patients because of its long-term repeated cycle in the adjuvant setting as well as in the metastatic setting. Current clinical studies have reported controversial data regarding cardiac safety when TRZ treatment and radiotherapy are given concur-

rently. Previous studies investigating the functioning change and mechanism of TRZ treatment in combination with irradiation are limited. Sridharan reported the fibrosis in rat hearts 6 months after receiving 21 Gy irradiation, which was also accompanied by the activation of neuregulin/HER-2 signaling. Such findings suggest that this signal pathway may be an important self-healing mechanism in cardiomyocytes that becomes activated in response to radiation injury [8]. Yavas et al. found that TRZ treatment combined with chest irradiation increased morphological abnormalities and functional damage of the cardiovascular system in rat models [9].

Our research group has long been committed to the clinical and basic research of cardio-oncology. Clinically, we reported an increased risk of acute left ventricular ejection fraction dysfunction and diastolic dysfunction in breast cancer patients who received radiotherapy and TRZ treatment when the radiation dose and volume were both increased [10]. Concurrent application of TRZ treatment also increased the risk of diastolic dysfunction in patients undergoing left chest wall radiotherapy [11]. In terms of basic research, we observed that TRZ combined with cardiac irradiation can cause early changes in cardiac function in mouse models [12].

In this study, we treated isolated cardiomyocytes with irradiation combined with TRZ, evaluated if this combination induces cardiomyocyte damage other than irradiation alone, and explored relevant molecular changes. We also investigated the effect of TRZ on late radiation-induced heart injury (6 months after radiation) using a mouse model and analyzed characteristic changes via imaging and histopathology.

Materials and methods

Animal experiment

All animal experiments and procedures were performed with the approval of the Shanghai Jiaotong University School of Medicine Institutional Animal Care and Use Committee. The animal model was conducted on male C57/BL6 mice (20-25 g, 4-6 weeks old) as described. Twenty mice were randomly assigned for four study groups: Control, IR, TRZ and IR+TRZ, respectively. The heart of animal was subjected to irradiation with 20 Gy/1Fx, 6 MV X ray, and the exposed field was localized at 1×1 cm^2, dose rate was 300 cGy/min, and source skin distance (SSD) was 100 cm. TRZ was administrated intraperitoneally (i.p.) to mice in two weeks (6 fractions) with a total dose at 10 mg/kg. The IR+TRZ group received heart irradiation next day with TRZ i.p. injection. The animal echocardiography and heart PET/CT was performed on 6 month later, and heart tissue were collected accordingly.

Mouse echocardiography

Using animal visual ultrasound imaging system with mouse probe (Sonic Vevo2100 and MS-400 probe), the mice were fixed on a thermostat in supine position and on electrodes coated with conductive agents in limbs. Superficial anesthesia was maintained with 1% isoflurane and oxygen. M-motion curves of left ventricular wall were collected, and at least 3 continuous and stable cardiac cycle images were collected and saved. Left ventricular M-mode motion curves were used to measure the ejection fraction (EF) and short axis systolic rate (FS). All data were averaged for three cardiac cycles. The flow of mitral valve orifice was observed by color Doppler ultrasound module, and the flow spectrum of mitral valve orifice was recorded by pulse spectrum Doppler module. The peak value of early diastolic blood flow (E peak) and late diastolic blood flow (A peak) were recorded. In Tissue Doppler Module, the myocardial motion spectrogram of the mitral annulus of the interventricular septum was collected, and the early diastolic velocity (E') and late diastolic velocity (A') of the mitral annulus were measured. The systolic function of cardiac function in mice was assessed by parameters LVEF and FS, and diastolic function was assessed by E/E'.

Mouse micro PET/CT

The small animal PET/CT system (SuperNova® PET/CT, PINGSENG Healthcare Inc.) was used to measure the uptake of ^{18}F-FDG by mouse cardiomyocytes. During scan acquisition, anesthesia in mice was maintained by 1.3% concentration of isoflurane. The PET image was reconstructed by OSEM algorithm, and the attenuation was corrected by referring to the CT image. Using avatar 1.5 software (Pingsheng healthcare Inc.), the heart was selected as the region

of interest (ROI) on the PET image, and the standard uptake value (SUV) of the heart was obtained by calculating the average radioactivity in ROI and the weight of mice.

Histological analysis

After the mice were sacrificed and perfused with PBS systemic circulation, the heart was quickly removed and fixed in 4% polyformaldehyde. The short-axis paraffin sections with 4 μm thickness were prepared by routine method for subsequent analysis. Cardiac morphology and myocardial fibrosis were evaluated in hematoxylin and eosin (HE) and Masson's stained sections, respectively. The apoptosis in the heart was detected by the TUNEL staining.

Cell culture and irradiation

Rat embryonic ventricular derived H9C2 cardiomyoblasts cells were purchased from the ATCC (CRL-1446, Rockville, MD, USA). The cells were irradiated by a medical linear accelerator (Varian Trilogy, FL, USA) with beam energy at 6-MV X-rays, dose rate at 300 cGy/ min; source-surface distance (SSD) at 100 cm. H9C2 cells were inoculated or with TRZ (5 ug/ml) in culture plates overnight, then exposure to IR at dose of 0, 2, 5, 10, 15 Gy.

Detection of cell apoptosis by flow cytometry

Apoptosis in cell culture was quantified with flow cytometry by staining cells with FITC-labeled Annexin V and Propidium Iodide (PI) (Invitrogen, Carlsbad, CA, USA). Briefly, at 48 h after simulated IR and/or treatment with TRZ, H9C2 cardiomyocytes were prepared to be incubated with FITC-labeled Annexin V and PI, and analyzed with a BD FACS Aria III flow cytometer (BD Biosciences, San Jose, CA, USA).

Cell viability

Cell viability was examined by CCK-8 assay (Beyotime, Shanghai, China). H9C2 cells were inoculated with TRZ in 96-well culture plates overnight, then exposed to IR. At 48 h after IR, the cells were assayed for cell viability in a humidified incubator at 37°C according to the manufacturer's instructions. The optical density was measured at 450 nm with a microplate reader (Synergy 2, BioTek, Winooski, VT, USA).

Western blot

At 48 h after simulated IR and/or treatment with TRZ, H9C2 cells were harvested for western blot analysis. Western blot analysis was performed by using antibodies for Bax (2772S, CST), Bcl2 (sc-7382, SANTA), p-AKT (13038, CST); β-actin (4970s; CST) or AKT (9272, CST) was used as internal control.

Gamma-H2AX foci formation

At 1 h after irradiation, cells were permeabilized with 0.3% Triton X-100-PBS, then blocked with 3% BSA, and followed by incubation in γ-H2AX antibody (CY6572, Abways, 1:100) overnight with gentle shaking. After washing with PBS, γ-H2AX antibody was visualized with Alexa Fluor-label antibody. Nuclei were counterstained with DAPI in PBS. The fluorescence intensity was observed under fluorescence microscopy (Zeiss AxioVert A1, Jena, Germany) and quantitated by using the ImageJ software (NIH, Bethesda, MD).

Detection of intracellular ROS

Intracellular ROS level was detected by a Reactive Oxygen Species Assay Kit (Beyotime Biotechnology, Shanghai, China). H9C2 cells with 1 μM of 2,7-dichlordihy-drofluorescein diacetate (DCFH-DA) at 37°C for 30 min in 6-well culture plates after treatment for 48 h. DCF fluorescence intensity was observed by flow cytometry (BD FACS Aria III).

Statistical analysis

The data are represented as the means ± SEM. Results were analyzed by one-way ANOVA and $P<0.05$ was defined as significant difference.

Results

Trastuzumab promotes irradiation induced apoptosis of H9C2 cells

H9C2 cardiomyocytes were treated with X-ray irradiation (doses of 0, 2, 5, 10, and 15 Gy). Flow cytometric analysis of apoptosis in H9C2 cardiomyocytes showed that X-ray irradiation could significantly induce the apoptosis of H9-C2 cardiomyocytes, and the degree of apoptosis was dose-dependent (**Figure 1A**). Notably, TRZ treatment alone did not significantly induce

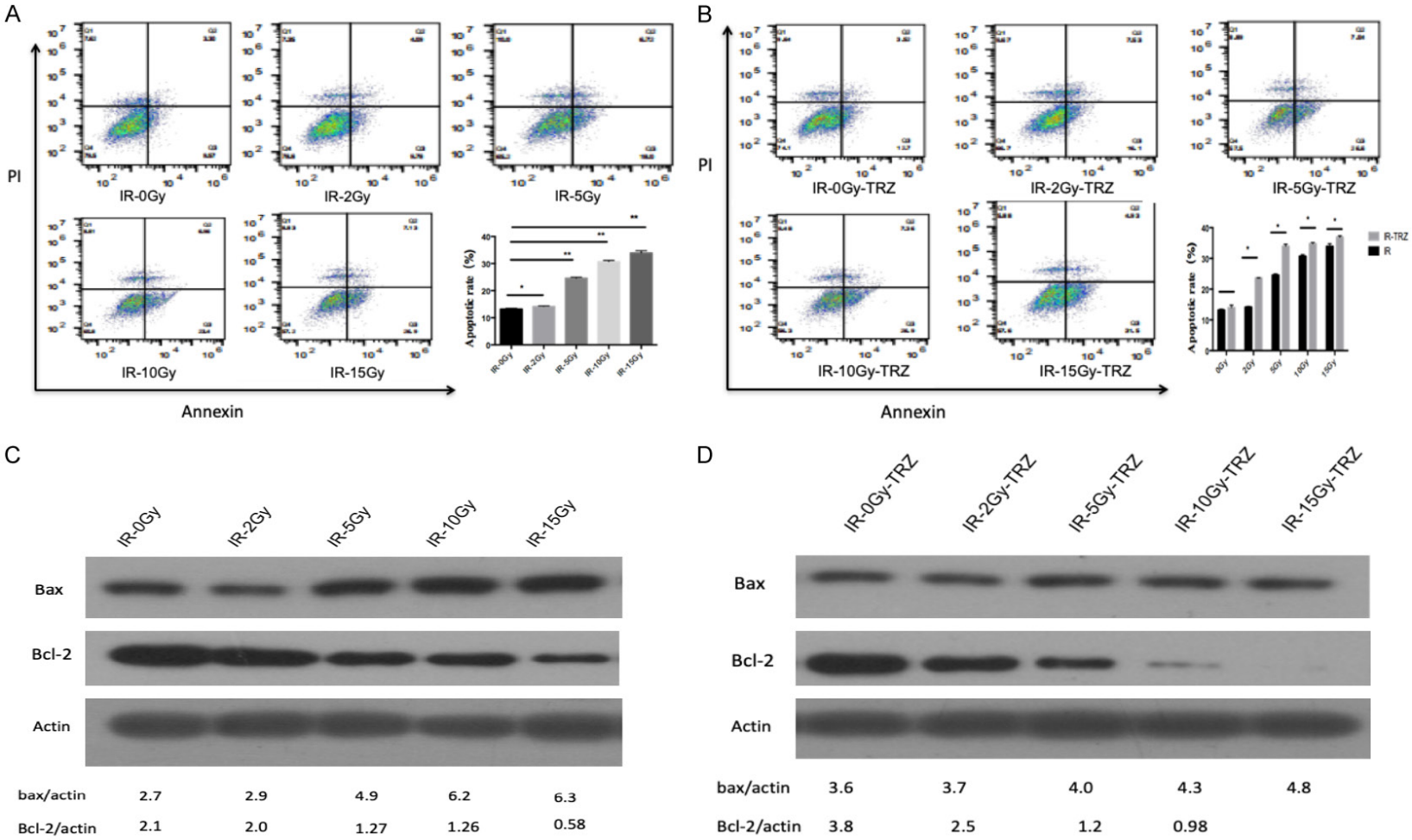

Figure 1. Trastuzumab promotes IR induced apoptosis of H9c2 cells. A. X-ray irradiation could significantly induce the apoptosis of H9c2 cardiomyocytes, and the degree of apoptosis was dose-dependent. And TRZ treatment alone did not significantly induce apoptosis in H9c2 cardiomyocytes. B. TRZ treatment alone did not significantly induce apoptosis in H9c2 cardiomyocytes. After adding TRZ treatment, TRZ could further aggravate radiation-induced apoptosis. C. The expression of Pro apoptotic protein Bax increased compared with the control group, while the expression of apoptosis inhibitory protein Bcl-2 decreased. D. After TRZ combined with irradiation, the expression of Bax protein also increased with the irradiation dose, while the expression of Bcl-2 decreased more significantly. $^{*}P<0.05$, $^{**}P<0.001$.

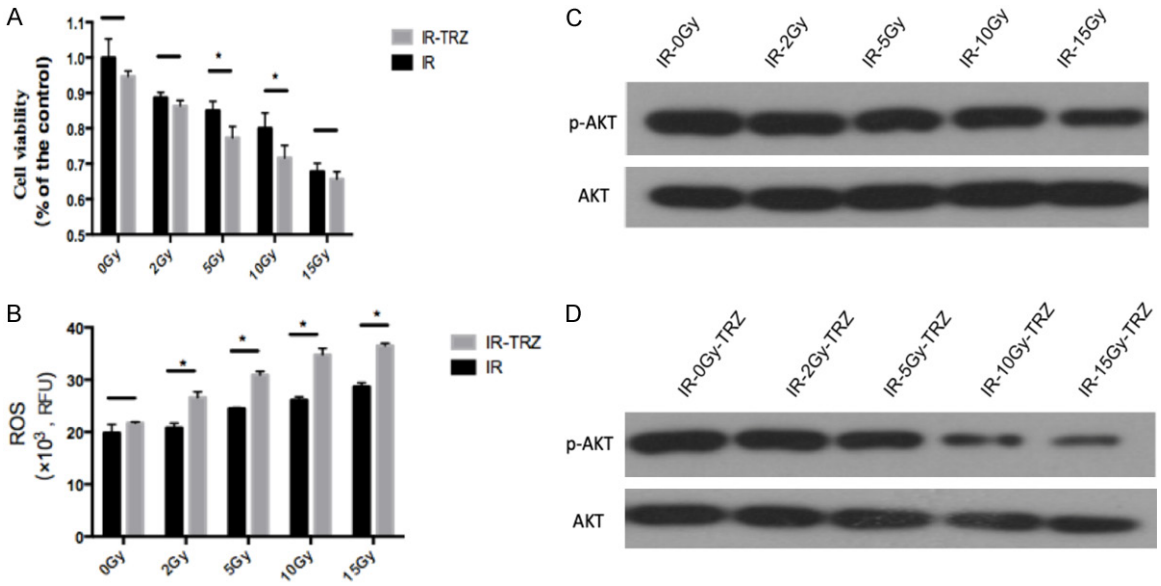

Figure 2. Effect of TRZ combined with irradiation on the viability, ROS and phosphorylation of Akt in H9c2 cells. A. Irradiation reduces the activity of cardiomyocytes, and the cell activity is further reduced after TRZ treatment. B. ROS content in cardiomyocytes was positively correlated with the irradiation dose. The application of TRZ will further increase the content of intracellular ROS. C. X-ray irradiation of H9c2 cardiomyocytes slightly inhibited the phosphorylation of Akt. D. After TRZ was administered, the phosphorylation of Akt in cardiomyocytes was significantly inhibited.

apoptosis in H9c2 cardiomyocytes. The addition of TRZ treatment, applied concurrently with irradiation, further increased radiation-induced apoptosis (**Figure 1B**).

Western blots were used to detect the expression of apoptosis related proteins. After X-ray irradiation, the expression of the pro-apoptotic protein, Bax, increased as compared to the control group, and the expression of the apoptosis inhibitory protein, Bcl-2, decreased (**Figure 1C**). The results indicated that X-ray irradiation can cause cardiomyocyte apoptosis in a dose-dependent manner. After TRZ was given with irradiation, the expression of Bax also increased with the irradiation dose, and the Bcl-2 decreased more significantly. These findings suggest that TRZ can promote cardiomyocyte apoptosis (**Figure 1D**).

The effect of TRZ combined with irradiation on ROS production and the viability of H9C2 cells

The effect of TRZ and X-ray irradiation on cardiomyocyte activity was analyzed by the CCK-8 test. The results showed that X-ray irradiation could significantly reduce the cellular activity of H9C2 cardiomyocytes (**Figure 2A**). Treatment with TRZ alone did not significantly affect the activity of cardiomyocytes. Moreover, in the low dose irradiation group (2 Gy), the simultaneous application of TRZ did not impact myocardial activity. When the irradiation dose was greater than 5 Gy, cell activity was significantly lower in the group simultaneously treated with TRZ than in that of the irradiation-only treated group. In summary, the CCK-8 test suggests that irradiation reduces the activity of cardiomyocytes, and that cell activity is further reduced after TRZ treatment.

Reactive oxygen species (ROS) are important mediators of cell damage induced by irradiation. In our study, intracellular ROS content was detected by dichloro-dihydro-fluorescein diacetate staining. We found that the ROS content in cardiomyocytes was positively correlated with the irradiation dose (**Figure 2B**), which was consistent with the increasing levels of irradiation causing increasing amounts of cell damage. The application of TRZ further increased the levels of intracellular ROS when irradiation was also applied; however, TRZ alone did not increase ROS levels.

TRZ inhibits the phosphorylation of Akt in irradiated H9C2 cells

The activation of the phosphatidylinositol 3 kinase/protein kinase B (PI3K/Akt) signaling

pathway enables cells to resist oxidative stress-related injury. We found that X-ray irradiation of H9c2 cardiomyocytes slightly inhibited the activation of Akt in H9c2 cells (as indicated by the decrease in Akt phosphorylation), which indicates impairment of a cell's ability to self-repair in response to irradiation (**Figure 2C**). After TRZ administration, the activation of Akt in cardiomyocytes was significantly inhibited (**Figure 2D**). The PI3K/Akt signaling pathway, which is downstream of HER-2, also plays a role in its physiological function. TRZ blocks the HER-2 signaling pathway, which results in the significant inhibition of Akt phosphorylation. The combination of TRZ and irradiation synergistically inhibited the phosphorylation of Akt and resulted in more damage. Because of the self-healing ability of the impaired cells was influenced.

TRZ promotes irradiation induced DNA damage in vitro

DNA is a key target of ionizing radiation. The ratio of γ-H2AX foci in cells correlated with the degree of intracellular DNA damage. We detected the effects of irradiation and TRZ on cardiomyocyte DNA damage by measuring γ-H2AX foci formation. As indicated in **Figure 3A**, X-ray irradiation (dose ≥5 Gy) could lead to γ-H2AX foci, and the fluorescence intensity was positively correlated with the irradiation dose. We analyzed the effect of TRZ combined irradiation on cardiomyocyte DNA damage. The results showed that when TRZ was administered with irradiation, the degree of DNA damage was further enhanced (**Figure 3B**).

The effect of irradiation and TRZ co-treatment on the physical condition of mice

After 6 months of cardiac irradiation and TRZ treatment, the body weight (**Figure 4A**) and heart weight (**Figure 4B**) of mice did not significantly change. However, the heart/body weight ratio decreased significantly in the irradiation group (control vs IR, 0.004974 vs 0.004127, $P<0.05$) and in the combined group (control vs IR+TRZ, 0.004974 vs 0.004455, $P<0.05$) (**Figure 4C**). There was no significant difference in heart/body weight ratio between the IR group and the combined group. Previous studies have found that irradiation can destroy melanocytes in hair follicles and lead to hair whitening [13]. We also observed hair whitening on the backs of irradiated mice, and the position and size corresponded to the area where irradiation was applied (**Figure 4D**).

Systolic and diastolic function as measured by echocardiography

Six months after heart irradiation, echocardiography showed that the diastolic function of the combined group had decreased significantly compared with the control group (control vs IR+TRZ, 20.66 vs 33.57, $P<0.05$); however, there was no significant abnormality in the irradiation-only group and TRZ group compared with the control group (**Figure 5**). No significant changes in systolic function in the parameters of EF and FS were observed between experimental groups (**Figure 6**).

Late radiation-induced heart disease (RIHD) is characterized by progressive myocardial ischemia, hypoxia, and myocardial fibrosis. Under normal conditions, one third of the myocardial energy supply comes from glucose and other comes from fatty acids. Under hypoxic conditions, the utilization of fatty acids by cardiomyocytes is limited and then the glycolytic pathway is enhanced, which improves the uptake of glucose. Based on this, the analysis of myocardial glucose uptake can reflect the state of myocardial injury. The level of myocardial injury in mice was detected by ^{18}F-Fluorodeoxyglucose micro-positron emission tomography/computed tomography (^{18}FDG micro-PET/CT), and the injury state of cardiomyocytes was reflected by the standardized uptake value (SUV). The uptake rate of FDG showed that irradiation could significantly increase the SUV of the heart (control vs IR, 0.5417 vs 1.235, $P<0.05$) (**Figure 7A**), and the SUV of the heart was further increased after TRZ treatment (IR vs IR+TRZ, 1.235 vs 1.829, $P<0.05$) (**Figure 7B**).

Myocardial fibrosis and cardiomyocyte apoptosis in mouse model hearts

The heart tissue in the combined group showed obvious structural disorder, thickening of the interstitial vascular wall, lumen stenosis, and local vacuolar degeneration (black arrow) and inflammatory cell infiltration (yellow arrow), as demonstrated by hematoxylin and eosin staining. The irradiation group showed moderate damage and the TRZ group was comparable to the control group, with no obvious abnormalities (**Figure 8A**).

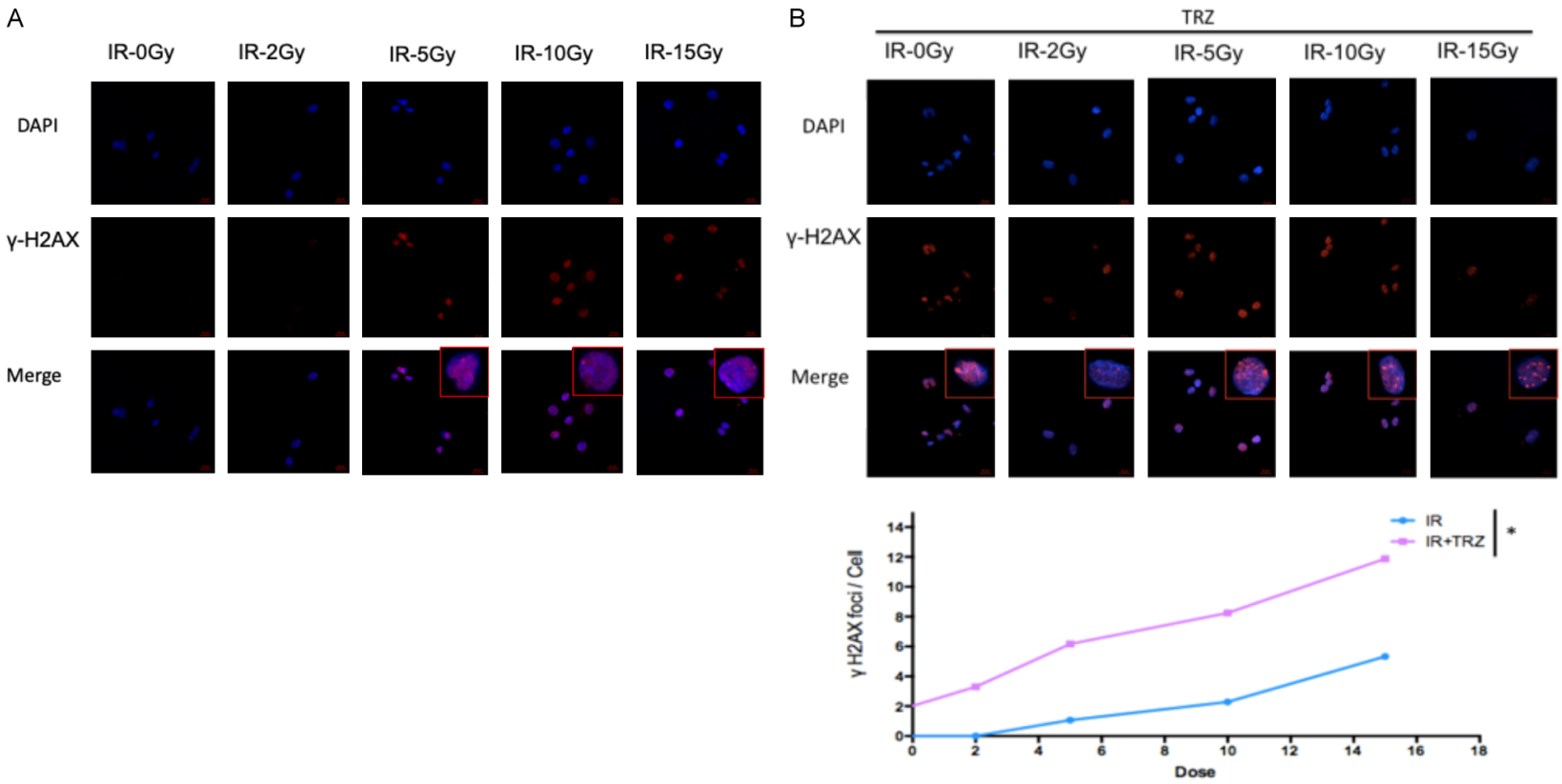

Figure 3. TRZ promotes irradiation induced DNA damage in vitro. The ratio of γ-H2AX foci in cells was correlated with the degree of intracellular DNA damage. A. X-ray irradiation (dose ≥5 Gy) can lead obvious γ-H2AX foci, and the fluorescence intensity was positively correlated with the irradiation dose. B. After TRZ was delivered with irradiation, the degree of DNA damage was further enhanced.

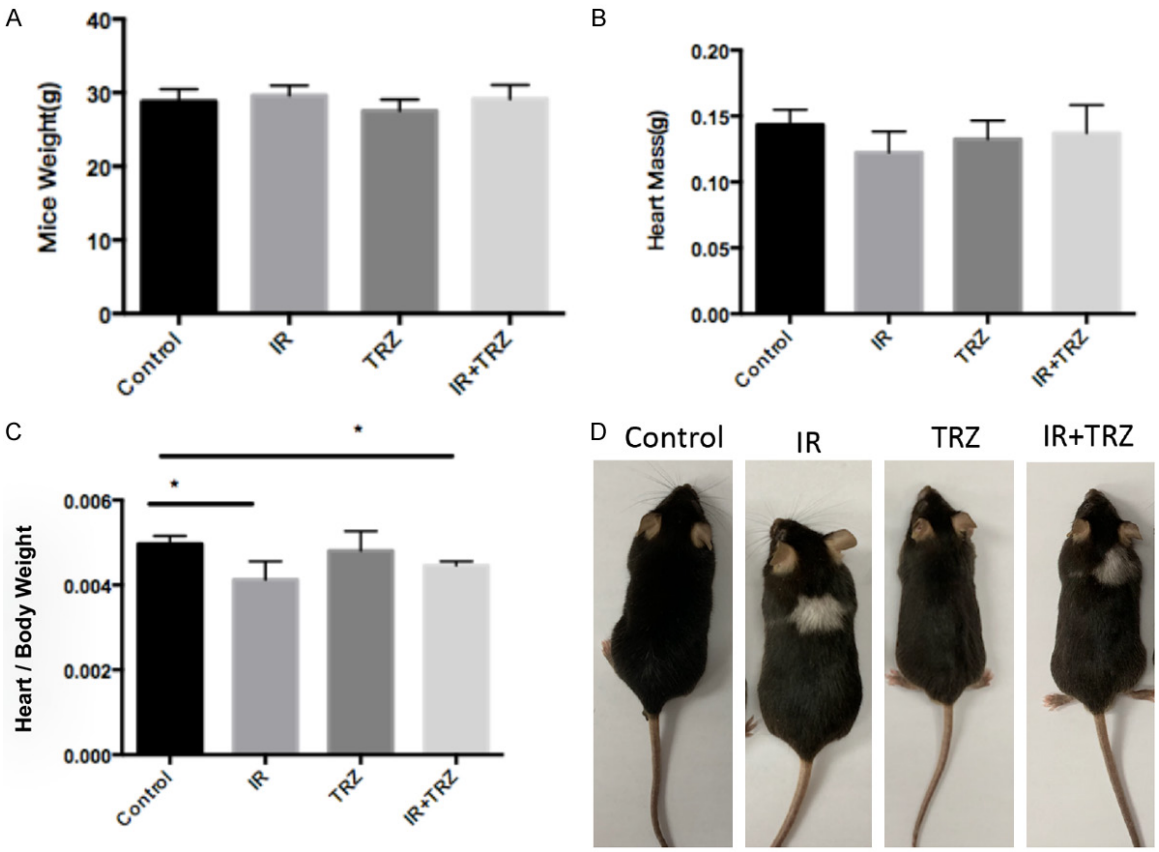

Figure 4. Irradiation and TRZ co-treatment on physical condition of mice. A, B. After 6 months of cardiac irradiation and TRZ treatment, the body weight and heart weight of mice were measured. C. The heart/body weight ratio decreased significantly in the irradiation group (control vs IR, 0.004974 vs 0.004127, $P<0.05$) and the combined group (control vs IR+TRZ, 0.004974 vs 0.004455, $P<0.05$). D. Hair whitening on the back of irradiated mice, and its position and size correspond to the chest radiation.

The myocardial fibrosis is characteristic of late RIHD and can be used to evaluate the degree of cardiac injury. Collagen deposition was observed in the perivascular and interstitial tissues of the left ventricle of the irradiation group and the combined group (**Figure 8B**). The presence of fibrosis in the combined group was more obvious than that of the irradiation-only group. No obvious fibrosis was observed in the TRZ and control groups.

Apoptosis in heart tissue was detected by utilizing TUNEL staining. The results showed that irradiation or TRZ treatment alone did not cause apoptosis in the heart; however, irradiation and TRZ combined resulted in apoptosis in heart tissue (**Figure 9**).

Discussion

Cardiomyocytes represent a critical component of the heart and are critical for the heart to maintain its physiological function. The classic radiobiological perspective holds that cardiomyocytes lacking proliferative ability and belong to a relatively radiation-resistant cell group. Cardiomyocyte damage caused by ionizing radiation primarily results from cell ischemia and hypoxia induced by damaged cardiac nutrient vessels [14]. Recent studies have found that direct injury of myocardial cells by irradiation is also an important factor in cardiac radiation injury. Ionizing radiation can produce irreparable DNA breaks in cardiomyocytes, which lead to further cell cycle inhibition or death [15, 16]. Additionally, irradiation can increase the expression of apoptosis related proteins, such as Bax/BCL, in cardiomyocytes and promote cardiomyocyte apoptosis [17]. The p53 molecule exerts protective effects on cardiomyocytes. Some studies have found that DNA damage and oxidative stress, induced by irradiation, can inhibit the activation of the p53.

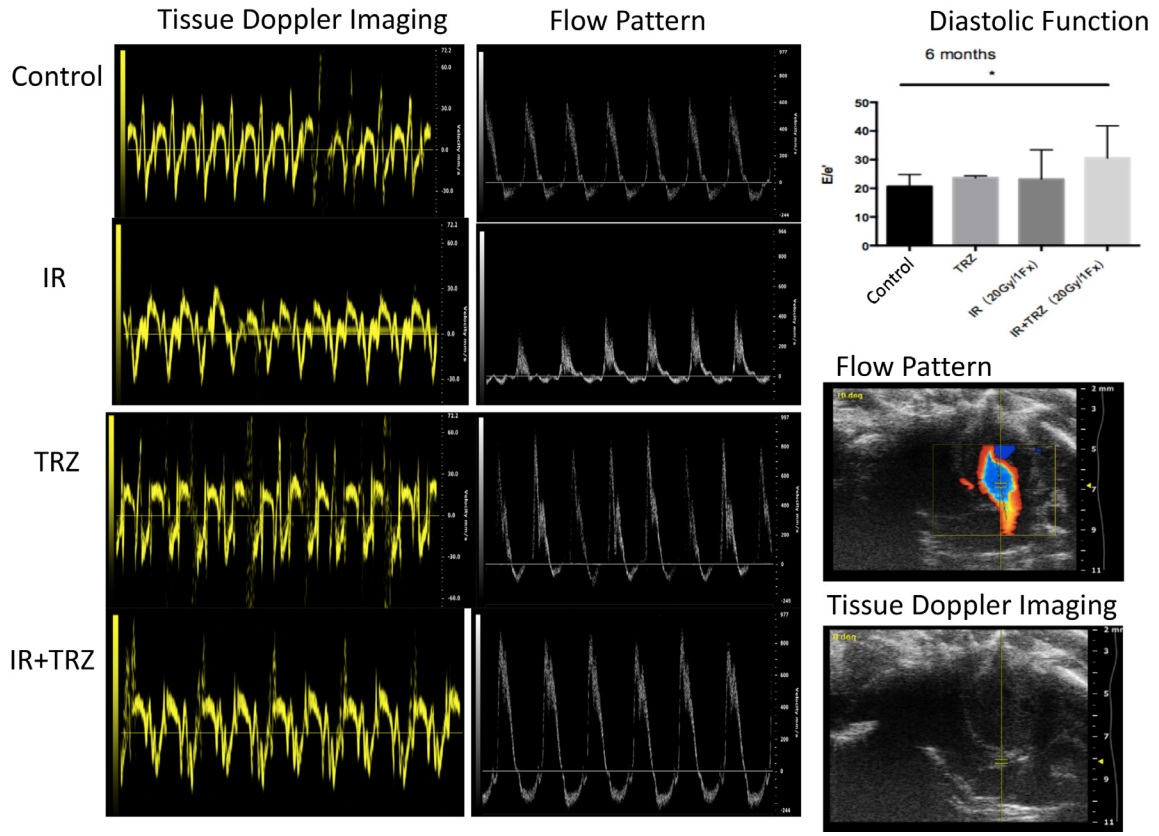

Figure 5. The effect of irradiation combined with trastuzumab on the diastolic function of mice. Six months after heart irradiation, the diastolic function was detected by echocardiography. The diastolic function of the combined group decreased significantly compared with the control group (control vs IR+TRZ, 20.66 vs 33.57, $P<0.05$). No significant abnormality in the irradiation-only group and TRZ group compared with the control group.

Considering this, irradiation may reduce the defense ability of cardiomyocytes against external stimuli by inhibiting the activation of p53 [18, 19]. Low linear energy transfer radiation, such as X-rays commonly used in the clinic, mainly exerts its effects by indirectly ionizing water molecules to produce ROS. It has also been reported that ROS can directly cause cardiomyocyte hypertrophy and even contribute to apoptosis at a cellular level [20]. Moreover, Puente et al. reported that ROS also had an impact on the development and regeneration of cardiomyocytes. Ionizing radiation inhibited the proliferative cycle of cardiomyocytes and affected the self-repair of damaged myocardium [21]. Although the adult myocardium loses most of its proliferative capability, a small number of cardiomyocytes do retain this function. Younger individuals contain a larger content of proliferative cardiomyocytes [22, 23], which explains why the same irradiation dose is more damaging to younger individuals than older individuals [24]. Taken together, this suggests that cardiomyocyte injury derived from ionizing radiation is an important factor.

Under physiological conditions, HER-2 plays an important role in the occurrence and development of the myocardium and the maintenance of cardiac function. Treatment with TRZ can reduce the expression of protective genes in mouse cardiomyocytes. The function of these genes includes maintaining normal myocardial function, DNA damage repair, and adaptability to stress stimulation [25]. After HER-2 activation, it mainly functions through the mitogen-activated protein kinase [26] and PI3K/Akt pathways [27, 28]. The activation of PI3K/Akt, as indicated by Akt phosphorylation (p-Akt), can regulate the respiratory state of mitochondria, reduce the production of ROS, and promote cell survival [29]. In cardiac tissue, the activation of HER2-PI3k/Akt signaling is also critical for regulating the normal physiological

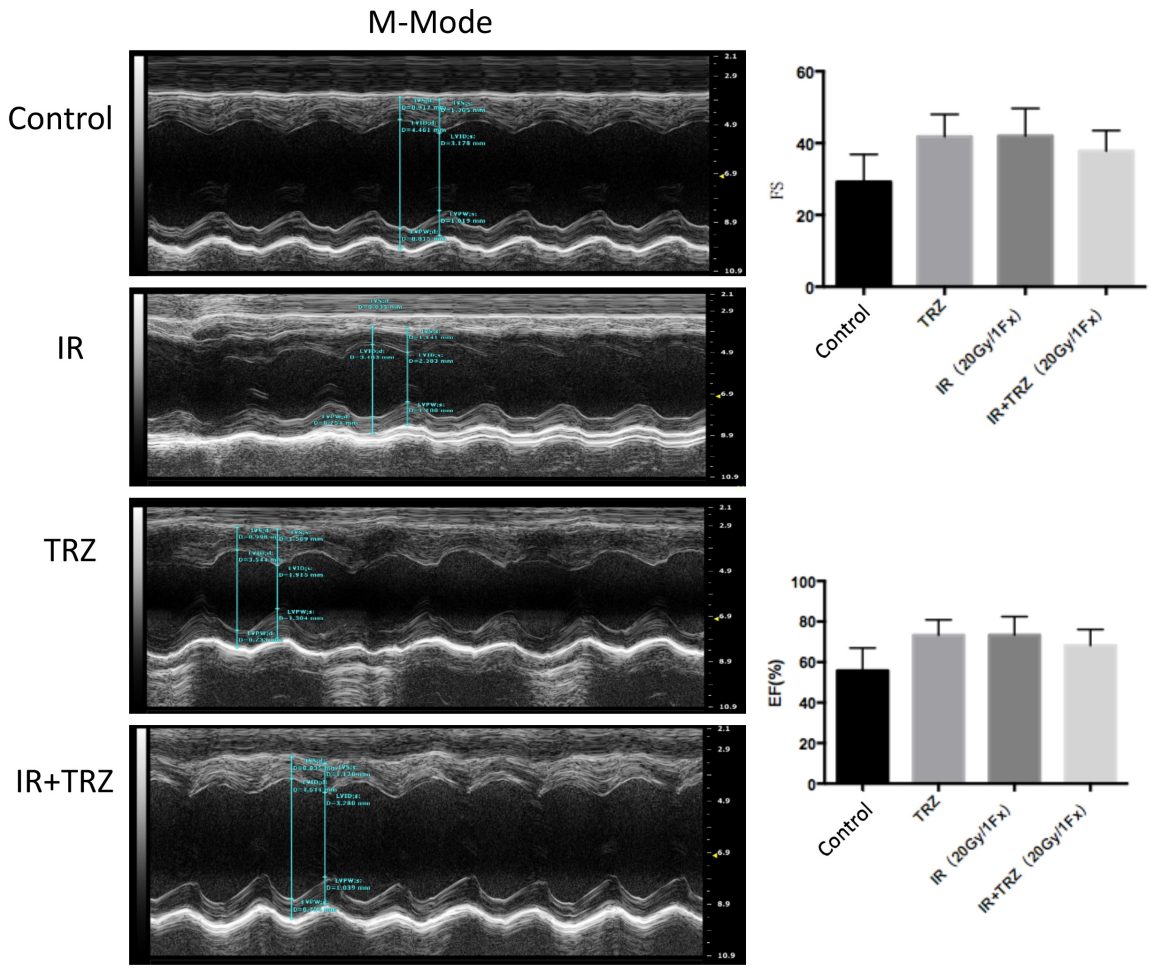

Figure 6. The effect of irradiation combined with trastuzumab on the systolic function of mice. Six months after heart irradiation, no significant changes in systolic function in parameters of LVEF (Left Ventricular Ejection Fractions) and FS (Fraction Shortening) were observed in all experimental groups compared with the control group.

state of the heart and helping to maintain the survival state of cardiomyocytes [30]. When HER-2 signal is blocked by TRZ, the maintenance of cardiomyocyte function and its defenses against harmful stimuli are significantly affected, which results in heart injury. By analyzing the damage mechanisms of X-ray irradiation and TRZ treatment on cardiomyocytes, we identified an intersection between the two damage mechanisms, which is also the theoretical basis of this study. Through in vitro experiments, we found that the simultaneous application of TRZ and irradiation superimposes the damage onto H9c2 cardiomyocytes. The related internal changes include the accumulation of intracellular ROS, DNA damage, increases in apoptosis, and reduced activity of cardiomyocytes.

Basic research studies suggest that HER-2 knockout mice spontaneously have diastolic dysfunction of cardiomyocytes and of the heart itself [31]. In a previous clinical study, our group reported that the simultaneous application of TRZ could increase the incidence of diastolic dysfunction in patients with left chest wall radiotherapy [10, 11]. These findings are consistent with the results of echocardiography in small animals in this study, which suggests that the abnormality of diastolic function (rather than systolic function) may be a more sensitive index of cardiac injury induced by radiotherapy combined with TRZ. This data also suggests that reporting diastolic function in the monitoring of cardiac toxic events by echocardiography would be of great significance.

Echocardiography is a commonly used imaging methodology for cardiac evaluation; however, cardiac ultrasounds may not be sensitive enough to detect RIHD because its accuracy is

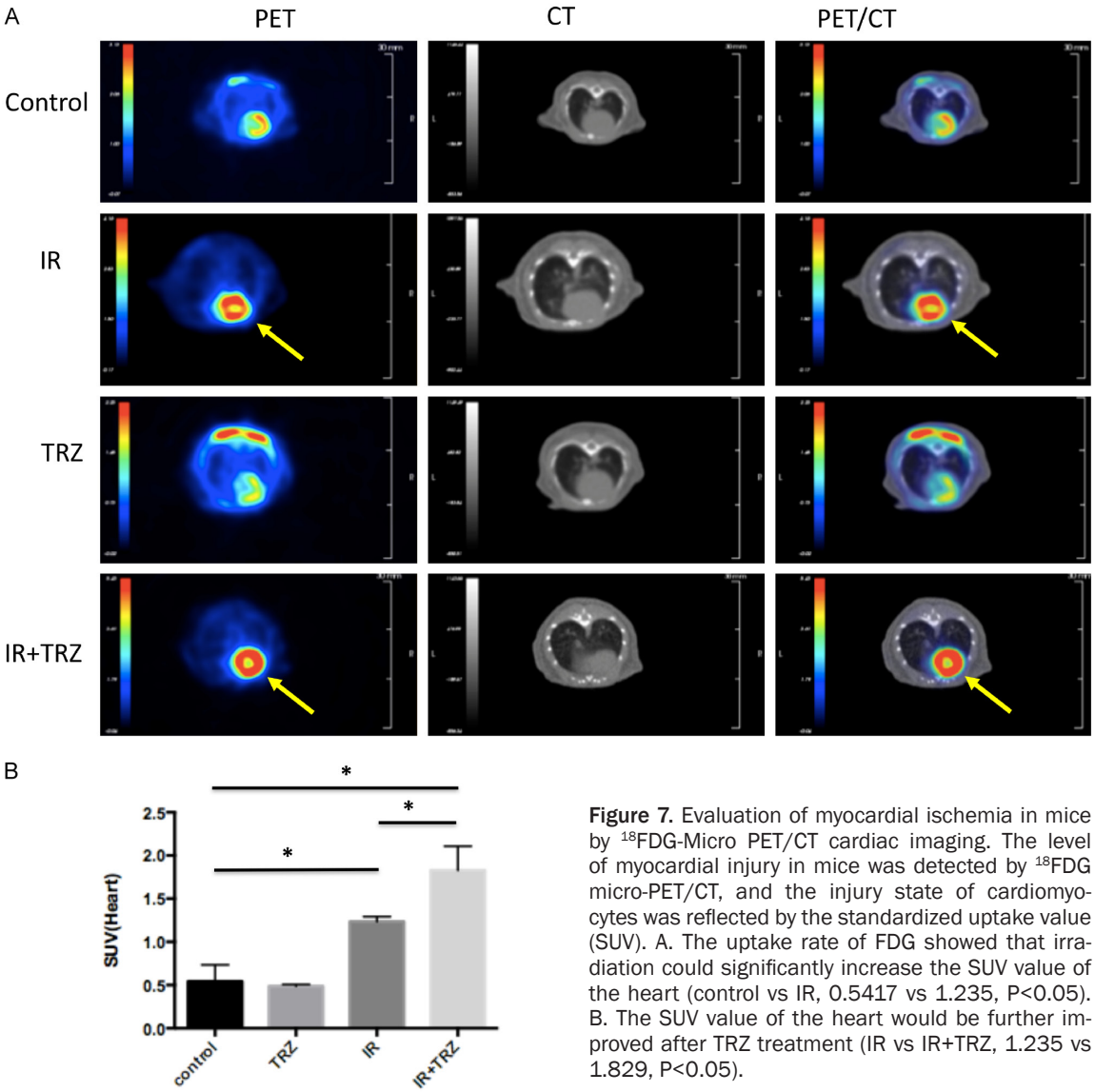

Figure 7. Evaluation of myocardial ischemia in mice by ^{18}FDG-Micro PET/CT cardiac imaging. The level of myocardial injury in mice was detected by ^{18}FDG micro-PET/CT, and the injury state of cardiomyocytes was reflected by the standardized uptake value (SUV). A. The uptake rate of FDG showed that irradiation could significantly increase the SUV value of the heart (control vs IR, 0.5417 vs 1.235, $P<0.05$). B. The SUV value of the heart would be further improved after TRZ treatment (IR vs IR+TRZ, 1.235 vs 1.829, $P<0.05$).

highly dependent on the technical skill of the operator and has poor repeatability [32]. It is also difficult to diagnose RIHD via echocardiography in cases with myocardial ischemia without abnormal cardiac function [33]. The detection of myocardial ischemia by ^{18}FDG-PET/CT has attracted the attention of researchers [34, 35]. Researchers from Japan found that patients with esophageal cancer, who had received chest radiotherapy, had increased myocardial ^{18}FDG uptake during ^{18}FDG-PET/CT; however, the mechanism of this uptake is not clear [36]. Kawamura found that after the heart was irradiated, uptake of FDG increased, and the area of increased FDG uptake also coincided with the irradiated area of the heart [37]. Chinese scholars explored the application of PET/CT in a canine RIHD model and found that there was high FDG uptake in the irradiated area of the canine heart, and the SUV was positively correlated with the degree of heart injury [38]. The mechanism of increased glucose uptake by the myocardium after irradiation may be explained by the fact that under physiological conditions of blood flow and oxygen supply, one third of the energy supplied to the myocardium comes from glucose and two thirds comes from the aerobic metabolism of fatty acids [39]. When aerobic respiration of the myocardium is affected, for example by insufficient blood and oxygen supply to the heart or mitochondrial respiratory dysfunction in cells caused by irradiation, the aerobic respiration of cardiomyocytes can be blocked. This in turn increases

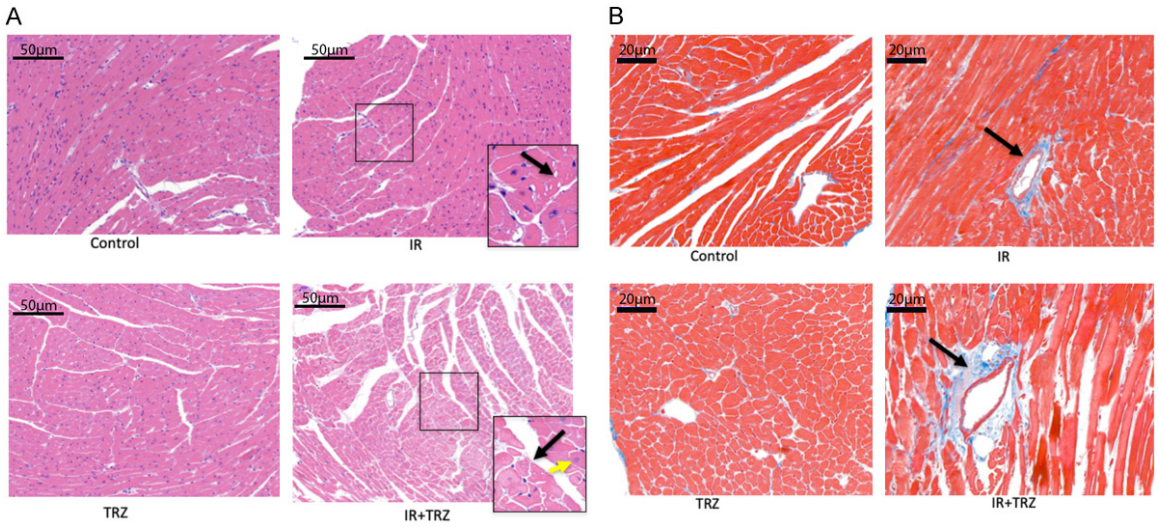

Figure 8. The HE and Masson staining in mouse heart. A. The heart tissue in the combined group showed obvious structural disorder, thickening of interstitial vascular wall, lumen stenosis, and local vacuolar degeneration (black arrow) and inflammatory cell infiltration (yellow arrow). The tissue of irradiation group showed moderate damage; and no obvious abnormality was found in TRZ or control group. B. Collagen deposition was observed in the perivascular and interstitial tissues of the left ventricle in the irradiation group and the combined group. The fibrosis in the combined group was more obvious than that in the irradiation group. No obvious fibrosis was observed in TRZ group and control group.

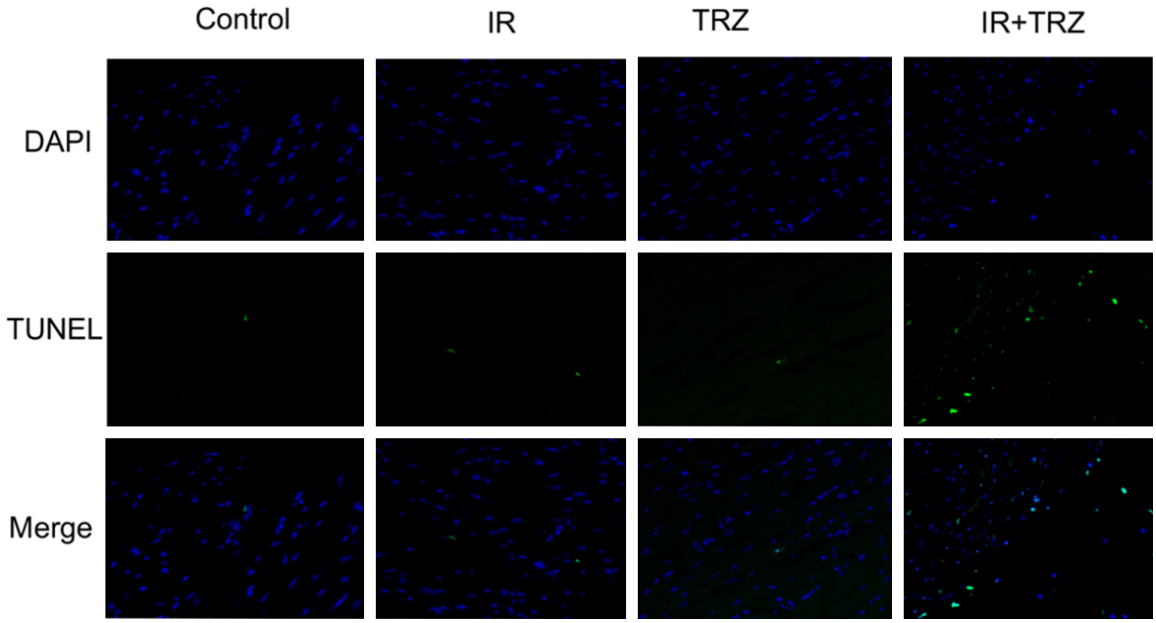

Figure 9. The detection of cardiomyocyte apoptosis by TUNEL in mouse heart. Irradiation or TRZ treatment alone could not cause obvious apoptosis in the heart; obvious apoptosis could be observed under the concurrent treatment of irradiation and TRZ.

the energy supply of anaerobic fermentation, resulting in increased glucose uptake and FDG uptake. Therefore, the FDG uptake rate reflects the degree of cardiomyocyte injury and could be used as an early detection method of RIHD.

Based on the results of the echocardiography (**Figures 5** and **6**), we found that diastolic dysfunction in sixth month after radiotherapy occurred only the in the combined group not in the irradiation alone group. However, the

results of the micro-PET/CT showed that the cardiac SUV increased in both the irradiation-only group and the combined group (**Figure 7**), although the increase in the SUV was more pronounced in the combined group. PET/CT may be more sensitive for detecting cardiac injury compared to echocardiography, especially when myocardial ischemia is present without obvious pumping dysfunction.

Conclusion

Concurrent administration of TRZ aggravates cardiomyocyte injury induced by irradiation. Treatment with TRZ might facilitate the radiation damage of the myocardium by inhibiting Akt phosphorylation and promoting the excessive accumulation of ROS in cells and intracellular DNA damage. The combination of small animal echocardiography and ^{18}FDG micro-PET/CT allowed for the early diagnosis of heart injury. Our study also had some limitations, such as this is a basic research, and the inner mechanism needs to be further explored. Our results do suggest that extra caution should be paid when concurrent use of TRZ and radiotherapy is indicated in clinical practice. More clinical data and better strategy is needed to optimize the treatment of radiotherapy and TRZ.

Acknowledgements

This study was supported in part by the National Key Research and Development Program of China (grant number 2016YFC0105409), Clinical Research Plan of SHDC (grant number SHDC2020CR2052B, SHDC2020CR4070), Scientific and Technological Innovation Action Plan of Shanghai Science and Technology Committee (grant number 19411950900, 19411950901), the Interdisciplinary Program of Shanghai Jiao Tong University (grant number ZH2018QNA54), National Natural Science Foundation of China (grant number 81702601, 81803164, 81972963), Special construction of integrated Chinese and Western medicine in general hospital (grant number ZHYY-ZXYJHZX-2-201913).

Disclosure of conflict of interest

None.

Address correspondence to: Min Li and Lu Cao, Department of Radiation Oncology, Ruijin Hospital, Shanghai Jiaotong University School of Medicine, 197 Ruijin er Road, Shanghai 200025, China. E-mail: lm11866@rjh.com.cn (ML); caolu_163@ymail.com (LC)

References

[1] Baskar R, Lee KA, Yeo R and Yeoh KW. Cancer and radiation therapy: current advances and future directions. Int J Med Sci 2012; 9: 193-199.

[2] Castellino SM, Geiger AM, Mertens AC, Leisenring WM, Tooze JA, Goodman P, Stovall M, Robison LL and Hudson MM. Morbidity and mortality in long-term survivors of Hodgkin lymphoma: a report from the childhood cancer survivor study. Blood 2011; 117: 1806-1816.

[3] van Leeuwen FE and Ng AK. Long-term risk of second malignancy and cardiovascular disease after Hodgkin lymphoma treatment. Hematology Am Soc Hematol Educ Program 2016; 2016: 323-330.

[4] Virani SA, Dent S, Brezden-Masley C, Clarke B, Davis MK, Jassal DS, Johnson C, Lemieux J, Paterson I, Sebag IA, Simmons C, Sulpher J, Thain K, Thavendiranathan P, Wentzell JR, Wurtele N, Cote MA, Fine NM, Haddad H, Hayley BD, Hopkins S, Joy AA, Rayson D, Stadnick E and Straatman L. Canadian cardiovascular society guidelines for evaluation and management of cardiovascular complications of cancer therapy. Can J Cardiol 2016; 32: 831-841.

[5] Daher IN, Daigle TR, Bhatia N and Durand JB. The prevention of cardiovascular disease in cancer survivors. Tex Heart Inst J 2012; 39: 190-198.

[6] Genuino AJ, Chaikledkaew U, The DO, Reungwetwattana T and Thakkinstian A. Adjuvant trastuzumab regimen for HER2-positive early-stage breast cancer: a systematic review and meta-analysis. Expert Rev Clin Pharmacol 2019; 12: 815-824.

[7] Seidman A, Hudis C, Pierri MK, Shak S, Paton V, Ashby M, Murphy M, Stewart SJ and Keefe D. Cardiac dysfunction in the trastuzumab clinical trials experience. J Clin Oncol 2002; 20: 1215-1221.

[8] Sridharan V, Sharma SK, Moros EG, Corry PM, Tripathi P, Lieblong BJ, Guha C, Hauer-Jensen M and Boerma M. Effects of radiation on the epidermal growth factor receptor pathway in the heart. Int J Radiat Biol 2013; 89: 539-547.

[9] Yavas G, Yildiz F, Guler S, Sargon MF, Yildiz D, Yolcu T, Tuncer M and Akyol FH. Concomitant trastuzumab with thoracic radiotherapy: a morphological and functional study. Ann Oncol 2011; 22: 1120-1126.

[10] Cao L, Hu WG, Kirova YM, Yang ZZ, Cai G, Yu XL, Ma JL, Guo XM, Shao ZM and Chen JY. Potential impact of cardiac dose-volume on acute cardiac toxicity following concurrent trastuzumab and radiotherapy. Cancer Radiother 2014; 18: 119-124.
[11] Cao L, Cai G, Chang C, Miao AY, Yu XL, Yang ZZ, Ma JL, Zhang Q, Wu J, Guo XM and Chen JY. Diastolic dysfunction occurs early in HER2-positive breast cancer patients treated concurrently with radiation therapy and trastuzumab. Oncologist 2015; 20: 605-614.
[12] Yi P, Li H, Fang Y, Su J, Xu C, Cao L, Li M and Chen J. Administration of trastuzumab with heart irradiation induced acute cardiotoxicity in mice. Am J Cancer Res 2020; 10: 536-544.
[13] Kinoshita K, Ishimine H, Shiraishi K, Kato H, Doi K, Kuno S, Kanayama K, Mineda K, Mashiko T, Feng J, Nakagawa K, Kurisaki A, Itami S and Yoshimura K. Cell and tissue damage after skin exposure to ionizing radiation: short- and long-term effects after a single and fractional doses. Cells Tissues Organs 2014; 200: 240-252.
[14] Paris F, Fuks Z, Kang A, Capodieci P, Juan G, Ehleiter D, Haimovitz-Friedman A, Cordon-Cardo C and Kolesnick R. Endothelial apoptosis as the primary lesion initiating intestinal radiation damage in mice. Science 2001; 293: 293-297.
[15] Gavrilov B, Vezhenkova I, Firsanov D, Solovjeva L, Svetlova M, Mikhailov V and Tomilin N. Slow elimination of phosphorylated histone gamma-H2AX from DNA of terminally differentiated mouse heart cells in situ. Biochem Biophys Res Commun 2006; 347: 1048-1052.
[16] Firsanov D, Vasilishina A, Kropotov A and Mikhailov V. Dynamics of gammaH2AX formation and elimination in mammalian cells after X-irradiation. Biochimie 2012; 94: 2416-2422.
[17] Salata C, Ferreira-Machado SC, De Andrade CB, Mencalha AL, Mandarim-De-Lacerda CA and de Almeida CE. Apoptosis induction of cardiomyocytes and subsequent fibrosis after irradiation and neoadjuvant chemotherapy. Int J Radiat Biol 2014; 90: 284-290.
[18] Lee CL, Moding EJ, Cuneo KC, Li Y, Sullivan JM, Mao L, Washington I, Jeffords LB, Rodrigues RC, Ma Y, Das S, Kontos CD, Kim Y, Rockman HA and Kirsch DG. p53 functions in endothelial cells to prevent radiation-induced myocardial injury in mice. Sci Signal 2012; 5: ra52.
[19] Mitchel RE, Hasu M, Bugden M, Wyatt H, Hildebrandt G, Chen YX, Priest ND and Whitman SC. Low-dose radiation exposure and protection against atherosclerosis in ApoE(-/-) mice: the influence of P53 heterozygosity. Radiat Res 2013; 179: 190-199.
[20] Sawyer DB, Siwik DA, Xiao L, Pimentel DR, Singh K and Colucci WS. Role of oxidative stress in myocardial hypertrophy and failure. J Mol Cell Cardiol 2002; 34: 379-388.
[21] Puente BN, Kimura W, Muralidhar SA, Moon J, Amatruda JF, Phelps KL, Grinsfelder D, Rothermel BA, Chen R, Garcia JA, Santos CX, Thet S, Mori E, Kinter MT, Rindler PM, Zacchigna S, Mukherjee S, Chen DJ, Mahmoud AI, Giacca M, Rabinovitch PS, Aroumougame A, Shah AM, Szweda LI and Sadek HA. The oxygen-rich postnatal environment induces cardiomyocyte cell-cycle arrest through DNA damage response. Cell 2014; 157: 565-579.
[22] Bergmann O, Bhardwaj RD, Bernard S, Zdunek S, Barnabe-Heider F, Walsh S, Zupicich J, Alkass K, Buchholz BA, Druid H, Jovinge S and Frisén J. Evidence for cardiomyocyte renewal in humans. Science 2009; 324: 98-102.
[23] Tzahor E and Poss KD. Cardiac regeneration strategies: staying young at heart. Science 2017; 356: 1035-1039.
[24] Fidler MM, Reulen RC, Henson K, Kelly J, Cutter D, Levitt GA, Frobisher C, Winter DL and Hawkins MM; British Childhood Cancer Survivor Study (BCCSS) Steering Group. Population-based long-term cardiac-specific mortality among 34 489 five-year survivors of childhood cancer in great britain. Circulation 2017; 135: 951-963.
[25] ElZarrad MK, Mukhopadhyay P, Mohan N, Hao E, Dokmanovic M, Hirsch DS, Shen Y, Pacher P and Wu WJ. Trastuzumab alters the expression of genes essential for cardiac function and induces ultrastructural changes of cardiomyocytes in mice. PLoS One 2013; 8: e79543.
[26] Zabransky DJ, Yankaskas CL, Cochran RL, Wong HY, Croessmann S, Chu D, Kavuri SM, Red Brewer M, Rosen DM, Dalton WB, Cimino-Mathews A, Cravero K, Button B, Kyker-Snowman K, Cidado J, Erlanger B, Parsons HA, Manto KM, Bose R, Lauring J, Arteaga CL, Konstantopoulos K and Park BH. HER2 missense mutations have distinct effects on oncogenic signaling and migration. Proc Natl Acad Sci U S A 2015; 112: E6205-6214.
[27] Yuan TL and Cantley LC. PI3K pathway alterations in cancer: variations on a theme. Oncogene 2008; 27: 5497-5510.
[28] Klement GL, Goukassian D, Hlatky L, Carrozza J, Morgan JP and Yan X. Cancer therapy targeting the HER2-PI3K pathway: potential impact on the heart. Front Pharmacol 2012; 3: 113.
[29] Fan GC, Zhou X, Wang X, Song G, Qian J, Nicolaou P, Chen G, Ren X and Kranias EG. Heat shock protein 20 interacting with phosphorylated Akt reduces doxorubicin-triggered oxidative stress and cardiotoxicity. Circ Res 2008; 103: 1270-1279.
[30] Watanabe T, Sato K, Itoh F and Iso Y. Pathogenic involvement of heregulin-beta(1) in antiatherogenesis. Regul Pept 2012; 175: 11-14.

[31] Odiete O, Hill MF and Sawyer DB. Neuregulin in cardiovascular development and disease. Circ Res 2012; 111: 1376-1385.

[32] Lancellotti P, Nkomo VT, Badano LP, Bergler-Klein J, Bogaert J, Davin L, Cosyns B, Coucke P, Dulgheru R, Edvardsen T, Gaemperli O, Galderisi M, Griffin B, Heidenreich PA, Nieman K, Plana JC, Port SC, Scherrer-Crosbie M, Schwartz RG, Sebag IA, Voigt JU, Wann S and Yang PC; European Society of Cardiology Working Groups on Nuclear Cardiology and Cardiac Computed Tomography and Cardiovascular Magnetic Resonance; American Society of Nuclear Cardiology, Society for Cardiovascular Magnetic Resonance, and Society of Cardiovascular Computed Tomography. Expert consensus for multi-modality imaging evaluation of cardiovascular complications of radiotherapy in adults: a report from the European Association of Cardiovascular Imaging and the American Society of Echocardiography. J Am Soc Echocardiogr 2013; 26: 1013-1032.

[33] Stoodley PW, Richards DA, Meikle SR, Clarke J, Hui R and Thomas L. The potential role of echocardiographic strain imaging for evaluating cardiotoxicity due to cancer therapy. Heart Lung Circ 2011; 20: 3-9.

[34] Schelbert HR, Henze E, Phelps ME and Kuhl DE. Assessment of regional myocardial ischemia by positron-emission computed tomography. Am Heart J 1982; 103: 588-597.

[35] Abbott BG, Liu YH and Arrighi JA. [18F]Fluorodeoxyglucose as a memory marker of transient myocardial ischaemia. Nucl Med Commun 2007; 28: 89-94.

[36] Jingu K, Kaneta T, Nemoto K, Ichinose A, Oikawa M, Takai Y, Ogawa Y, Nakata E, Sakayauchi T, Takai K, Sugawara T, Narazaki K, Fukuda H, Takahashi S and Yamada S. The utility of 18F-fluorodeoxyglucose positron emission tomography for early diagnosis of radiation-induced myocardial damage. Int J Radiat Oncol Biol Phys 2006; 66: 845-851.

[37] Kawamura G, Okayama H, Kawaguchi N, Hosokawa S, Kosaki T, Shigematsu T, Takahashi T, Kawada Y, Hiasa G, Yamada T, Matsuoka H and Kazatani Y. Radiation-induced cardiomyopathy incidentally detected on oncology (18) F-fluorodeoxyglucose positron emission tomography. Circ J 2018; 82: 1210-1212.

[38] Yan R, Song J, Wu Z, Guo M, Liu J, Li J, Hao X and Li S. Detection of myocardial metabolic abnormalities by 18F-FDG PET/CT and corresponding pathological changes in beagles with local heart irradiation. Korean J Radiol 2015; 16: 919-928.

[39] Stanley WC, Recchia FA and Lopaschuk GD. Myocardial substrate metabolism in the normal and failing heart. Physiol Rev 2005; 85: 1093-1129.